#### **NURETH14-382**

# EFFECT OF HORIZONTAL FLOW ON THE COOLING OF THE MODERATOR BRICK IN THE ADVANCED GAS-COOLED REACTOR

P. Ganesan<sup>1</sup>, S. He<sup>2</sup>,\*, F. Hamad<sup>3</sup> and J. Gotts<sup>4</sup>

<sup>1</sup> University of Malaya, Kuala Lumpur, 50603, Malaysia

<sup>2</sup> University of Sheffield, Sheffield S1 3JD, UK

<sup>3</sup> University of Aberdeen, Aberdeen, AB24 3UE, UK

<sup>4</sup> EDF Energy, Nuclear Generation, Barnwood, Gloucester GL4 3RS, UK

poo ganesan@um.edu.my, \*s.he@sheffield.ac.uk, f.hamad@abdn.ac.uk, jim.gotts@edf-energy.com

#### **Abstract**

The paper reports an investigation of the effect of the horizontal cross flow on the temperature of the moderator brick in UK Advanced Gas-cooled Reactor (AGR) using computational fluid dynamics (CFD) with a conjugate heat transfer model for the solid and fluid. The commercial software package of ANSYS Fluent is used for this purpose. The CFD model comprises the full axial length of one-half of a typical fuel channel (assuming symmetry) and part of neighbouring channels on either side. Two sets of simulations have been carried out, namely, one with cross flow and one without cross flow. The effect of cross flow has subsequently been derived by comparing the results from the two groups of simulations. The study shows that a small cross flow can have a significant effect on the cooling of the graphite brick, causing the peak temperature of the brick to reduce significantly. Two mechanisms are identified to be responsible for this. Firstly, the small cross flow causes a significant redistribution of the main axial downward flow and this leads to an enhancement of heat transfer in some of the small clearances, and an impairment in others although overall, the enhancement is dominant leading to a better cooling. Secondly, the cross flow makes effective use of the small clearances between the key/keyway connections which increases the effective heat transfer area, hence increasing the cooling. Under the conditions of no cross flow, these areas remain largely inactive in heat transfer. The study shows that the cooling of the moderator is significantly enhanced by the cross flow perpendicular to the main cooling flow.

### 1. Introduction

In the UK Advanced Gas-cooled Reactor (AGR) design, graphite is used as the moderator and pressurized CO<sub>2</sub> as the coolant [1, 2]. The reactor core typically consists of over 300 fuel channels as shown in Fig. 1. In the centre of each fuel channel are clusters of 36 fuel pins, which are housed in graphite sleeves to form fuel elements. Eight fuel elements connected axially form a fuel assembly. These sit in cylindrical graphite moderator bricks as shown in Fig. 2. There are two vertical cooling passages for each moderator brick: One is on the bore of the brick, referred to as the annular passage (AnnP) and the other is on the outer surface of the brick, referred to as the arrowhead passage (AP). The name of AP comes from the shape of the passage (Fig. 2). The coolant flow is down through these two channels and up through the fuel cluster within the sleeve. In addition to the main moderator bricks, there are also connecting bricks, called interstitial bricks, sitting between the main graphite bricks (Fig 2). The graphite bricks are connected to each other through a radial key/keyway system on the outer surface of the bricks and small clearances of various sizes exist in these connections. Because of the pressure gradient that exists in the reactor core, there is a small horizontal cross flow from the

peripheral fuel channels to the inner fuel channels (see Fig. 1) through these key/keyways clearances. The effect of such flows on the cooling of the graphite brick is commonly considered to be insignificant in comparison with the cooling due to the axial downward flow and is therefore neglected in the calculations adopted by the industry. However there is a lack of understanding of the true effect.

The purpose of the present study is two folds: (i) to assess the effect of cross flow on brick temperature in an AGR core and (ii) to assess the uncertainties of the simple representation of cross flow used in the subchannel code PANTHER [5] that is currently used in the UK nuclear industry.

A commercial Computational Fluid Dynamic package is used in this study. Such methods have been widely used in many engineering applications, e.g., thermal-hydraulic analyses in a nuclear reactor [2, 3, 4]. In this paper, we will present a description of the physical model, followed by a discussion on the development of the CFD model. We will then present and discuss the modelling results using the CFD software package of Ansys Fluent followed by conclusions. The study is specifically carried out to understand the cross flow effect on brick temperature of Torness power station in UK but the result can be applicable to any Advanced Gas-cooled Reactor (AGR) plant, which has a cross flow (i.e., horizontal flow).

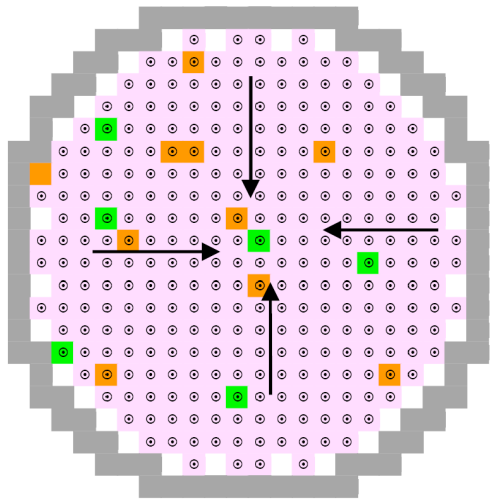


Figure 1: Top view of advanced gas cooled reactor (AGR). Arrows show the direction of the cross flow flowing from the outer to the inner moderator bricks.

## 2. Methodology

### 2.1 Description of the domain considered

A fuel channel in Ring 6 has been chosen to be the base channel for the CFD model. The CFD model includes a half channel of Ring 6 and 1/8 of the neighbouring channel (Ring 7) nearer the circumference of the AGR and 1/8 of the neighbouring channel (Ring 5) nearer the centre, see Fig. 2. The computational domain begins from the outer sleeve wall, covering the fluid flow through the annular passage (AnnP), models the conduction through the moderator main brick, and the fluid flow in the arrowhead passage (AP), and ends at the outer bound of arrowhead passage (i.e. the surface of the interstitial bricks). Re-entrant cooling fluid enters the domain and flows vertically from top to bottom through the annular passage and arrowhead passage. The total axial height considered for a channel is 8.32114m excluding the top and bottom headers of the reactor to cover the total height of all the fuel elements in the channel. There is a lateral leakage flow of coolant from the arrowhead flow

passage to the annular flow passage through inter-brick gaps at some AGR stations. However, such leakage is not significant in the context of the present study on the Torness AGR. The dimension of moderator brick of a nuclear reactor changes over the time. In the present study, the CFD model is based on Torness 'hot, start of life' (HOT SOL) dimensions [6].

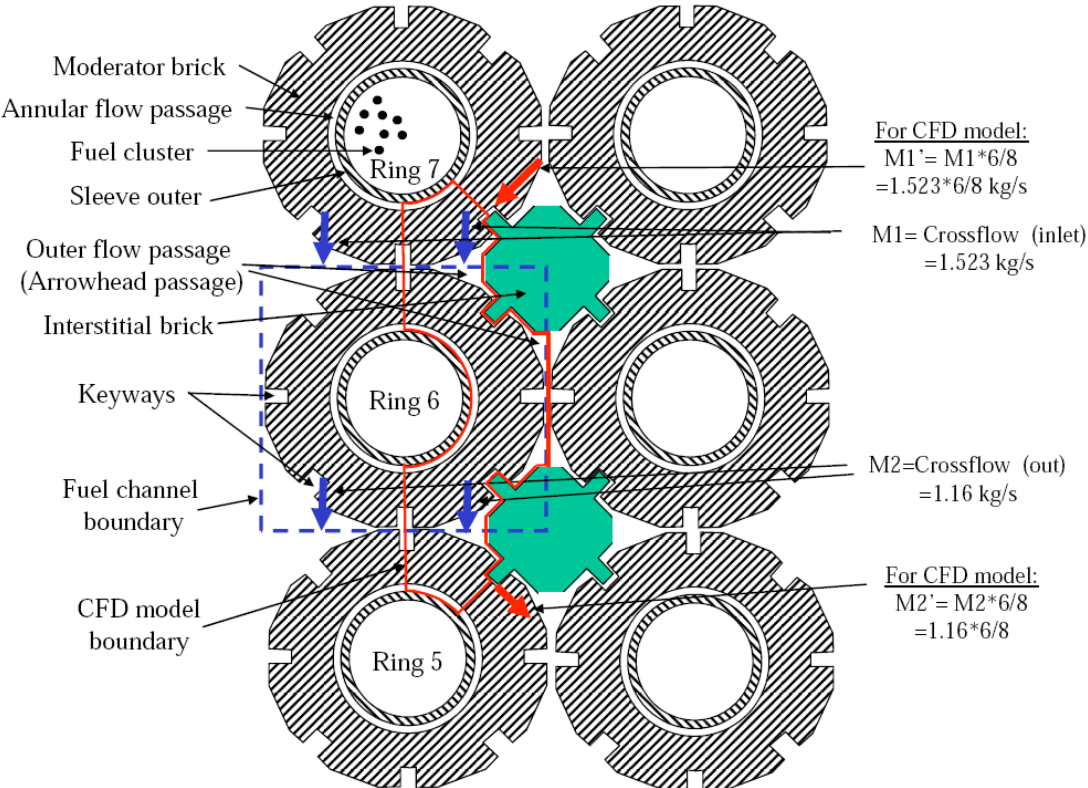


Figure 2: Top view of AGR fuel channels. In the centre of each fuel brick are fuel pins, which are surrounded by a graphite sleeve. The annular passage (AnnP) flow is formed in between of the sleeve outer wall and the moderator (brick) inner wall. The flow passage at the brick outer surface is referred to as arrowhead passage (AP). The boundary of the CFD model is shown in the figure.

### 2.2 Modelling

## 2.2.1 Brick and coolant modelling

The heat transfer in the moderator brick has been described using the thermal conductivity equation. The coolant flow in the annular passage (AnnP) and arrowhead passage (AP) have been described using the incompressible three-dimensional flow formulation of the Reynolds averaged momentum equations and the energy equation. Turbulence has been modelled using a 'standard' k- $\epsilon$  model. The heat transfer between the solid and fluid is coupled. The equations are discretized using the second order upwind spatial discretization.

### 2.2.2 Radiation modelling

The radiation is modelled using discrete transfer radiation model (DTRM), which is available in Fluent. The main assumption of DTRM is that the radiation leaving the surface element in a certain range of solid angles can be approximated by a single ray. The advantages of this model are: it is a relatively simple model, the accuracy of the model can be increased by increasing the number of rays and it applies to a wide range of optical thickness. The disadvantages are: the model assumes that all surfaces

## The 14<sup>th</sup> International Topical Meeting on Nuclear Reactor Thermalhydraulics, NURETH-14 Toronto, Ontario, Canada, September 25-30, 2011

are diffuse, the effect of scattering is not included, the implementation assumes gray radiation, and solving a problem with a large number of rays is CPU-intensive [7]. The radiation model is used for the AnnP with an emissivity value of 0.76 at both the outer sleeve surface and the inner brick surface. This is to be consistent with the value used in the Panther code AE.

## 2.2.3 Modelling of the rib-roughened sleeve wall

The annular outer sleeve consists of rectangular ribs with a height of 0.51 to 0.76 mm, and a width of 0.38 to 0.64 mm. The pitch (i.e., the distance of rib to rib) is 4.70 to 5.08 mm. The effect of the ribs is modelled using the Fluent rough wall boundary conditions. Parameters that need to be set for using this feature are the (sand-equivalent) roughness height and roughness constant [2]. But there are no obvious relationships between the rib roughness and these parameters. Through sensitivity study the roughness height and roughness constant were set as 1mm and 1, respectively, in Fluent. These values were obtained to ensure the total heat received by the annular gas flow in the Fluent model is the same as that obtained using Panther AE, which has been extensively validated against plant data.

#### 2 2 4 Mesh

The axial length of the domain is divided into 130 mesh elements with a bias towards the top and the bottom of the domain. For each radial cross section, there are about 17000 cells. The model typically has about 2.2 M elements. A structured mesh is used.

### 2.3 Simulation

In the reactor, the incoming cross flow (or lateral flow) from Ring 7 is greater than the outgoing one to Ring 5 in the arrowhead passage, resulting in an increase in the vertical flow down that passage. These cross flows are simulated using two methods. One is without explicitly considering the effect of the momentum of the cross flow on heat transfer, which will be referred to as no cross flow (NoCF) simulation, and one is with explicit consideration, which will be referred to as cross flow (CF) simulation.

### 2.3.1 'No cross flow (NoCF)' and 'Cross flow (CF)' models

The NoCF model simulates the simplified method used in PANTHER which only takes into consideration the increase of mass due to the imbalanced cross flow at the cross flow inlet/outlet, using a mass source, but the cross flow velocity is not simulated. Such a simulation was carried out by incorporating all the modelling aspects and boundary conditions of Panther AE into the CFD model so as to reproduce results from Panther AE. The 'cross flow' is considered only in terms of adding mass and energy as sources at three discreet regions of the axial height in the CFD model due to the difference between the incoming cross flow from Ring 7 and the outgoing cross flow to Ring 5. That is, the momentum of the cross flow is not considered.

The CF model intends to simulate the full effect of the cross flow. The incoming cross flow from Ring 7  $(m_1)$  and the outgoing one to Ring 5  $(m_2)$  are simulated using inlet and outlet velocity boundary conditions in Fluent. Uniform velocity distribution at the inlet/outlet are given, which are calculated based on the mass flow rate and flow area (A). This study is to investigate the effect of not considering cross flow velocity on brick temperature. The approximation in PANTHER method was then assessed by comparing the results from the CF and NoCF simulations.

## 2.4 Property and boundary conditions

## 2.4.1 Properties of the brick and CO<sub>2</sub>

The data for the thermal conductivity (k) as a function of temperature (T) of the un-irradiated graphite was obtained from Maruyama and Harayama [8]. For simplicity, k is represented using a two-point linear variation. The data used are: [T(K), k (W/mDegC)] = [586.89001 109.724] and [715.77301 98.576599]. The  $CO_2$  properties at a constant pressure of 4.45 MPa, which is an average pressure in Ring 6 channel, was generated using the NIST fluid property software. These data has been input to Fluent and linear interpolation is used in the CFD model.

## 2.4.2 Input data and boundary conditions

The input data condition for the CFD models are obtained from Panther AE. The data include: (i) non-uniform heat flux at sleeve outer surface (Q5); (ii) heat flux through the surface of interstitial brick forming the main arrowhead passage only (QAP), see Fig. 3; (iii) temperature and mass flow rate at the top inlet and bottom outlet of the Annular passage (AnnP) and Arrowhead passage (AP); (iv) the walls of the top and bottom brick are treated as adiabatic; and (v) direct heat generation in the brick.

### 3. Results and discussion

Several locations on the inner and outer surfaces were selected to show the axial variation of the temperature of the brick, referring to Fig. 3 (Left). 'In-top', 'In-mid' and 'In-bottom' are locations at the inner brick. 'Out-AH1', 'Out-AH3' and 'Out-AH4' are locations at the brick outer surfaces within the main arrowhead passage (MAP) of gas. 'Out-NG1', 'Out-NG2' and 'Out-NG3' are also locations at the outer brick locations, but, these locations are at the key/keyway clearances. Fig. 3 (Right) shows half of Ring 6 channel divided into 26 surfaces with the first 13 surfaces closer to incoming cross flow (or Ring 7). Surfaces 3, 4, 10, 11, 16, 17, 23 and 24 are brick surfaces at the main arrowhead passage, whereas the rest of surfaces are brick surfaces at the key/keyway clearances.

## 3.1 Brick temperature

Figs. 4(a) and 4(b) show the temperature contours over the horizontal cross section at an axial height of y = 4.158m down from the top of the model. for NoCF and CF simulations, respectively. Fig. 5 shows the axial variation of the temperature of the brick at several locations of NoCF and CF simulations, respectively. The difference between the two simulations is shown in Fig. 6. Figs. 7(a) and 7(b) show the comparison of the azimuthal variation of the temperature on the outer surface of the brick in the top and bottom quarter of the cross section of the brick at y=4m. The upper curves in 7a & 7b are the NoCF case. Figs. 7(c) and (d) show the difference between the brick surface temperature in the NoCF and CF simulations at y=4m.

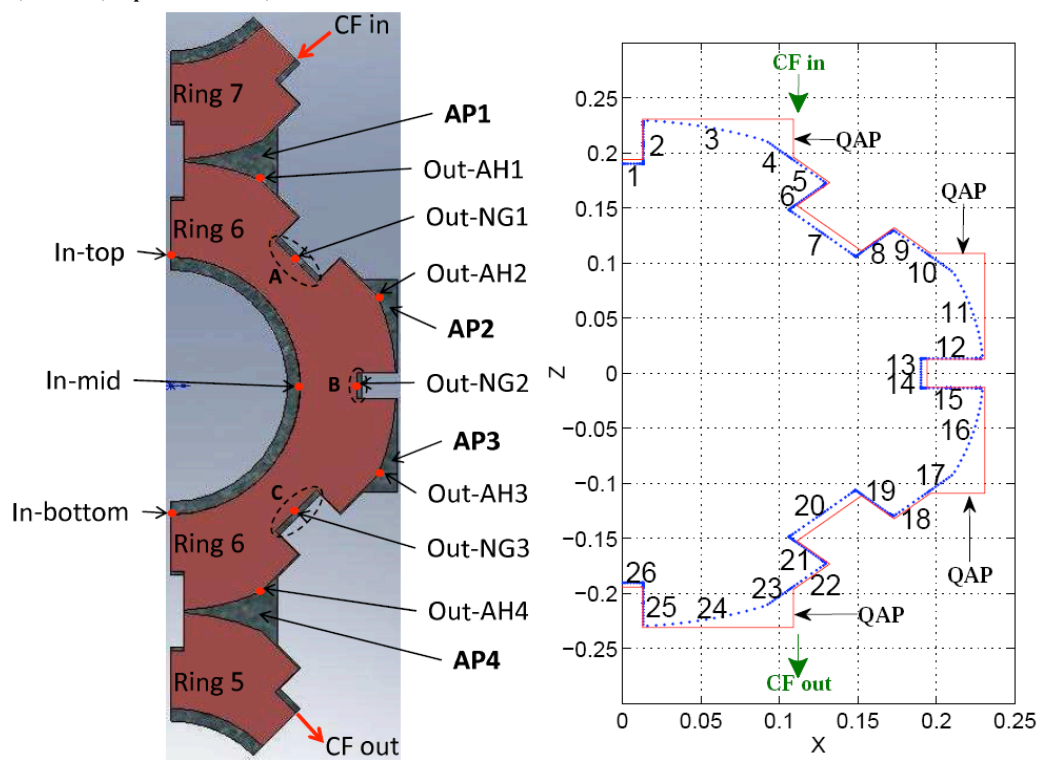


Figure 3: **Left:** Locations of the vertical lines used for result presentation of axial variation of brick temperature on the inner and outer surfaces. **Right:** Brick outer surfaces of Mid-Brick (Ring 6 channel) are classified into 26 surfaces for presenting results. The outer boundary surface of QAP, the heat flux through the interstitial brick for Ring 6 channel, is shown in the figure.

## 3.1.1 No Cross Flow (NoCF) simulation

For no cross flow (NoCF), the temperature distribution on any horizontal cross-section is reasonably axi-symmetric (Fig. 4a). Especially, there are very small azimuthal variations on the brick inner surface. This is also quantitatively shown in Fig. 5. The axial temperature profiles at the top, middle and bottom of the brick inner surfaces (i.e., In-top, In-mid and In-bottom) overlap each other. Only the temperature at In-Top is shown in the figure. There are two types of temperature distributions at the brick outer surfaces. For all locations at the main arrowhead passage (MAP), i.e., 'Out-AH1', 'Out-AH2', 'Out-AH3' and 'Out-AH4', the temperature also overlaps each other. Only the temperature at Out-AH1 is shown in the figure. The temperature at locations Out-NG1 (not shown), Out-NG2 and Out-NG3 (not shown) at the key/keyway clearances again overlaps each other but is much higher than that at locations in the MAP (Note: NG means narrow gap). There are two reasons for higher brick temperature at the key/keyway clearances than that at MAP; (1) the heat transfer coefficient is smaller in the narrow gaps than in the MAP (see later) and (2) there are less fluid and hence smaller cooling capacity in the NGs.

The temperature profile along the curvature of the brick outer surface at axial height 4m in NoCF is shown in Figs. 7(a) and 7(b). Starting from surface 1, the temperature gradually decreases with the increase of the curvature length. The lowest temperature is at the end point of surfaces 3 and 4 (in the MAP). Following that, the temperature increases with the increase of curvature length. The temperature peaks on surface 7. The temperature of surfaces 1 to 6 is symmetrical to that of surfaces 8 to 13 and also 14 to 26. In general, the temperature is higher at surfaces of the key/keyway clearances and lower at surfaces of the main arrowhead passages.

## The 14<sup>th</sup> International Topical Meeting on Nuclear Reactor Thermalhydraulics, NURETH-14 Toronto, Ontario, Canada, September 25-30, 2011

Compare the temperature profiles at the brick inner and outer surfaces of Panther AE and NoCF simulation by referring to Fig. 5. Note that AE1 and AE2 are the brick inner and outer surface temperatures from PANTHER. AE1 should be compared with In-Top and AE2 with the average value of Out-AH1 and Out-NG2. The agreement between the predictions of the brick temperature of the two models is reasonable although some discrepancies are clearly evident, with a maximum of about 10 °C at the axial height 4-5 m. These discrepancies result from the different modelling approaches of the CFD (Fluent) and the sub-channel (PANTHER). These differences are not significant for the purpose of the present study, which is based on the comparison between CF and NoCF modelling and not the absolute values.

## 3.1.2 Cross Flow (CF) simulation

For CF model, referring to Fig. 4(b), the temperature distribution is not axi-symmetric any more. Referring to the middle brick (i.e., Ring 6 channel), the temperature is generally speaking lower at the top of the figure and higher at the bottom. This has clearly resulted from the influence of the cross flow. The quantitative difference can be seen from Fig. 5. For example, the temperature is 15 °C higher at the bottom of the inner surface (i.e., In-bottom) than at the top of the inner surface (i.e., In-top) at y=6m. On the brick outer surface of the main arrowhead passage (MAP), the temperature is higher at Out-AH4 than at Out-AH1 with a difference of 22 °C at y=6m. In the NG, the temperature is higher in Out-NG3 than in Out-NG1 and Out-NG2 (not presented).

Referring to Figs. 7(a) and 7(b), the lowest temperature has now moved to faces 5 & 6 (and 11 & 12, and 18 & 19). That is the cooling of the narrow gap regions immediate downstream of the main arrowhead as far as the cross flow is concerned is significantly improved. On the other hand, the cooling in the last quarter (faces 21 - 26) is less efficient, which is consistent with the observation shown in the contour plot (Fig. 4(b)). The temperature at the bottom of the brick is relatively higher in CF. The temperature in key/keyway clearances can be lower than that in the main arrowhead passages.

### 3.1.3 Comparison of NoCF and CF simulations

Now, compare CF brick temperature with NoCF temperature, referring to Fig. 6, which show the temperature difference between NoCF and CF (i.e., NoCF minus CF). Overall the brick temperature predicted in the CF is clearly lower than that in the NoCF. The difference of the brick temperature increases as the gas flows down the channel, reaching the maximum around 4m to 6m and reduces afterwards. On both the inner and outer surfaces, the difference is higher at the top of the brick cross section and lowest at the bottom. The peak difference is 27 °C on the inner surface (In-Top), 32 °C next to the main arrowhead (Out-AH1) and >35 °C in the narrow gap (Out-NG1). All occur around 5m to 6m from the channel inlet. The least reduction occurs at the bottom of the cross section, being 10 °C max next to the main arrowhead (Out-AH4) and 15 °C max on the inner surface (In-Bot).

The difference between the brick surface temperature in NoCF and CF simulations, shown in Figs. 7(c) and 7(d), peaks on surfaces 5, 6, 11 and 12, which are located at the downstream of the cross flow of the MAP. It is also clear that the difference in NoCF and CF temperature is greater at the top of the brick cross section than at the bottom. Care needs to be taken to interpret this result. These are quite localised and have a relatively small impact on the overall brick temperature distribution. This information is very useful in understanding the enhanced cooling in CF but the practical impact in brick temperature needs to be based on an averaged view. Taking an averaged view, the temperature difference is about 35°C in the first and second quarter, 28°C in the third quarter and 16°C in the last quarter.

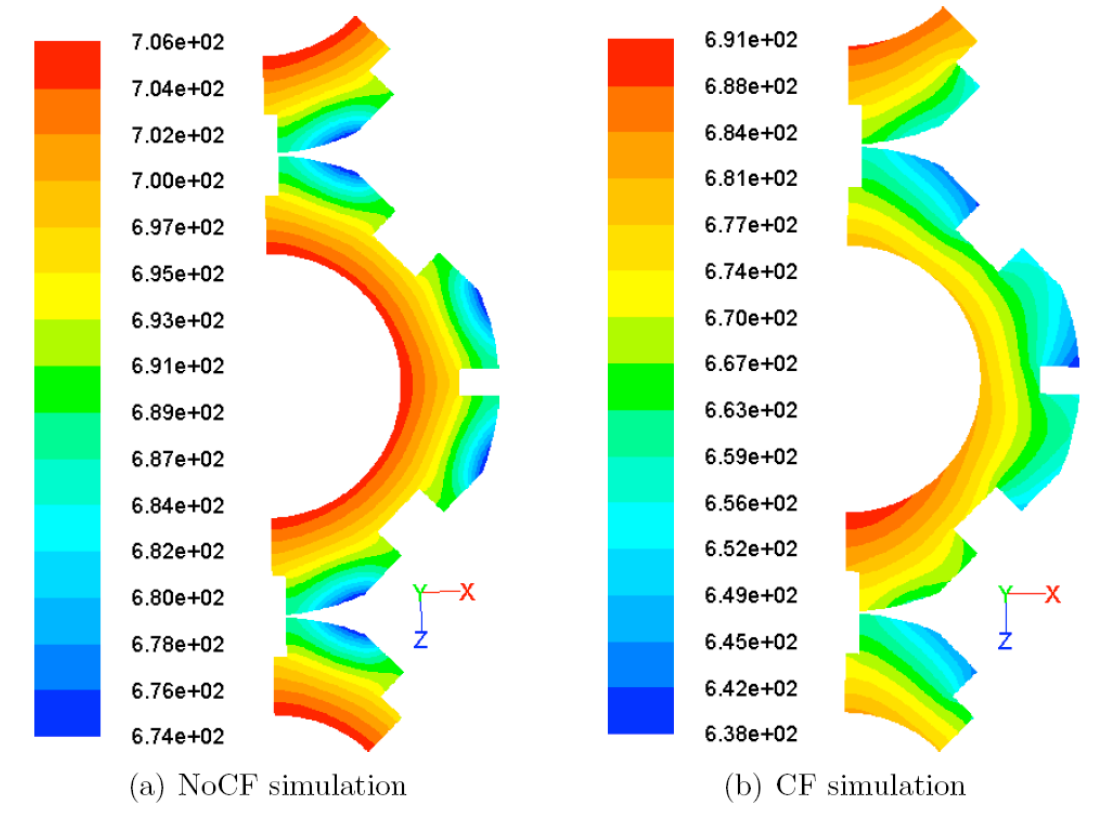


Figure 4: Temperature contours at axial height y=4.158m for (a) NoCF simulation; (b) CF simulation. Cross flow (CF) enters at the top and exits at the bottom of the figure.

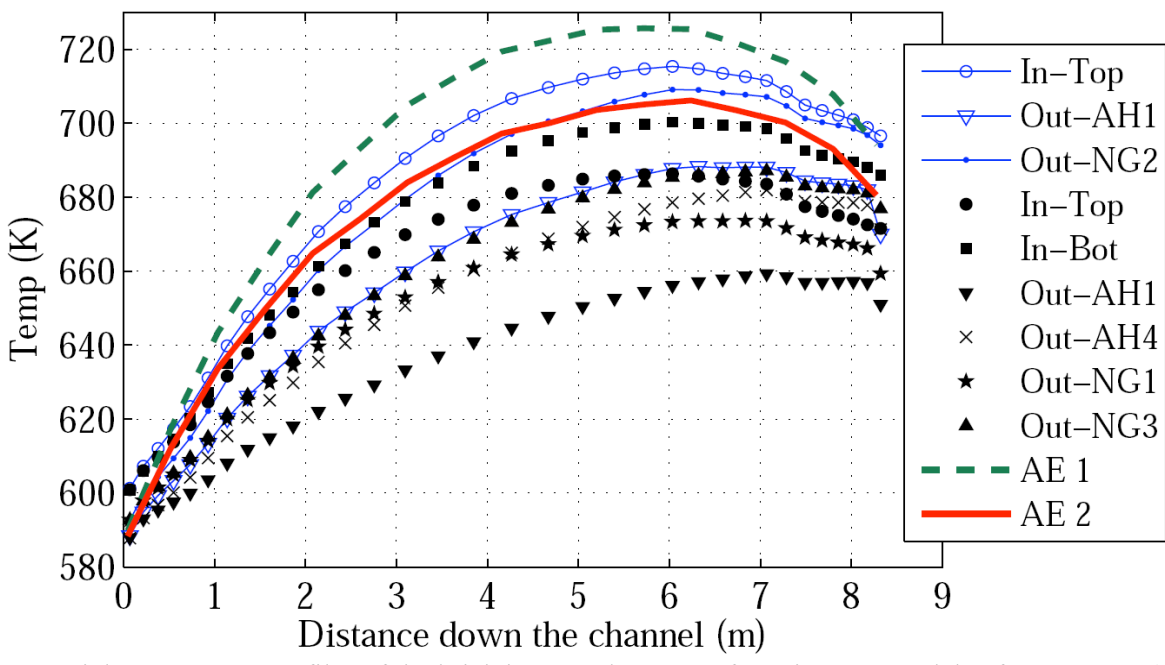


Figure 5: Axial temperature profiles of the brick inner and outer surfaces in CFD models of case NoCF (marker with solid line) and case CF (filled marker), and PANTHER (AE1 & AE 2). Refer to Fig. 3 for the locations.

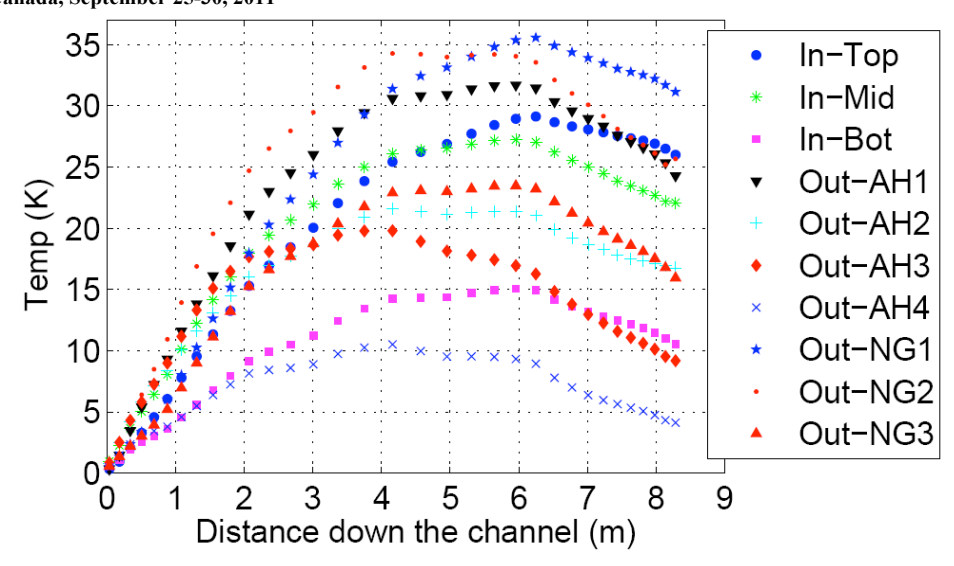


Figure 6: The temperature of case NoCF minus that of case CF of the results shown in Fig. 5.

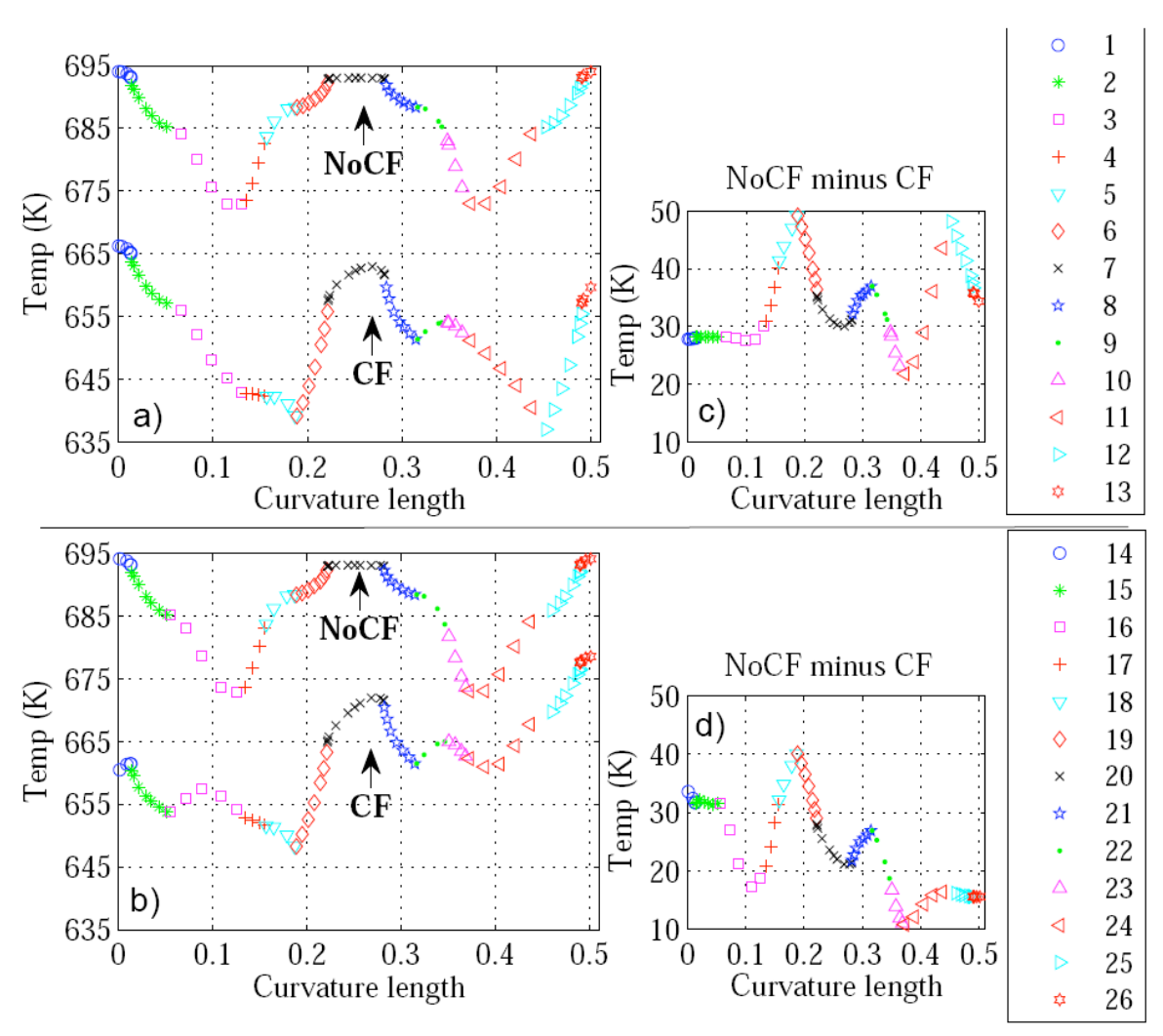


Figure 7: Wall temperature at an axial height of 4m along brick surface curvature for cases NoCF and CF of (a) top half of Mid-Brick [surfaces 1-13] and (b) the bottom half of Mid-Brick [surfaces 14-26], and the temperature difference of case NoCF minus case CF for surfaces (c) 1-13 and (d) 14-26.

### 3.2 Velocity distribution (Flow pattern)

Cross-sectional contours plots of the axial velocity  $(V_y)$  at axial height y=4.158m is shown in Figs. 8(a) and 8(b) for NoCF and CF simulations, respectively. The negative sign of the  $V_y$  indicates that the main flow is downwards. It can be seen from Fig. 8(a) that, for the NoCF case, the maximum axial velocity is at the centre of the arrowhead passage and the velocity distribution is symmetric. In the CF case (Fig. 8(b)) the location of the peak velocity is shifted towards one side of the arrowhead passage by the cross flow, which is from the top to bottom in Fig. 8(b). As a result, the axial velocity (and the heat transfer) is significantly increased on one side (away from the cross flow inlet) and reduced on the other side. This explains the low temperature on faces 5 and 6 and relatively high temperature on faces 23 to 26 discussed earlier.

The quantitative value of the axial velocity  $(V_y)$  near to brick surfaces 3 to 9 from top to bottom of the channel is shown in Fig. 9 for NoCF and CF simulations. For NoCF model, the axial velocity is highest at surfaces 3 or 4 (i.e., at main arrowhead passage), increasing gradually with the increase of the axial distance. For example, the velocity at the top and bottom of the channel is about -8 m/s and -13 m/s, respectively. However, for the rest of the locations (i.e., key/keyway clearances), the distribution of the velocity is quite uniform after 2 m from the top inlet. The flow readjusts itself within the first 2 m. Among various key/keyway clearances (faces 5 to 9), faces 6 and 8 has the lowest velocity. The magnitude of the velocity is directly dependent on the size of the key/keyway clearances. The larger the size is, the large the velocity.

For CF model, as a consequence of the velocity shift by cross flow shown in Fig. 8(b), the axial velocity at brick surfaces 3 to 9 has increased. An increase of nearly 3 times can be seen for the velocity near surface 5 (i.e., 3 m/s and 9 m /s for NoCF and CF simulations, respectively). Among these surfaces, the velocity near surface 7 has a small increase. This result shows that CF is capable of re-distributing the axial flow within the main arrowhead passage and also from the main passage to the key/keyways clearances.

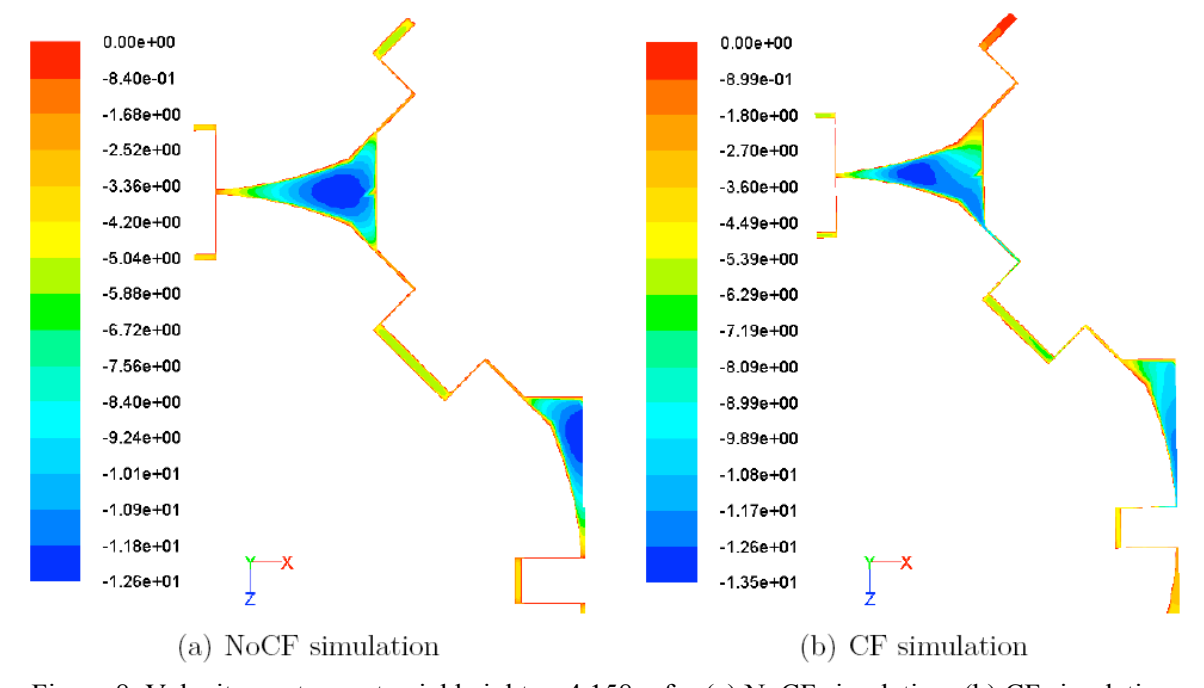


Figure 8: Velocity contours at axial height y=4.158m for (a) NoCF simulation; (b) CF simulation.

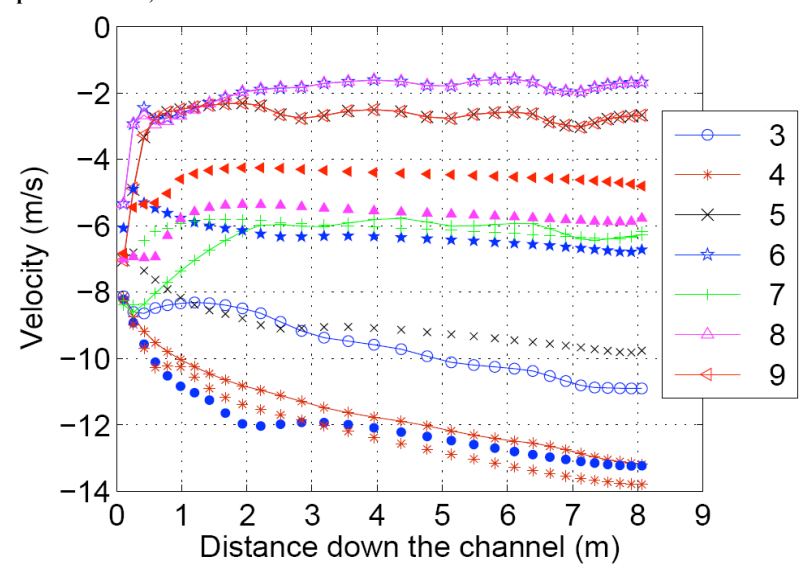


Figure 9: Velocity component of  $V_y$  of case NoCF (markers with solid line) and CF (markers only) of Faces 3 to 9.

## 3.3 Heat transfer coefficient

The heat transfer coefficient (h) for each brick outer surface is calculated using its local heat flux, local wall temperature and local coolant temperature in the AP near the brick surface. The axial variations of h for various brick surfaces for NoCF and CF simulations are shown in Fig. 10. For the NoCF case, h is highest in the main arrowheads (faces 3, 4 etc) being about 600 W/m<sup>2</sup>K. It is about 400 W/m<sup>2</sup>K on face 7 and between 300 W/m<sup>2</sup>K and 400 W/m<sup>2</sup>K on the faces 5 and 9. At the entry region (within the first 1m) h is much higher. h is significantly increased in all channels in CF as a result of cross flow. The value now ranges from 700 W/m<sup>2</sup>K to 1200 W/m<sup>2</sup>K for faces 3, 4, 5, 7 and 9. h on the narrow gap faces near the exit of the cross flow from the main arrowhead passages (e.g., surface 5) is significantly increased. This is consistent with the results of velocity, as the vertical flow has been pushed towards this side by the cross flow (and the maximum velocity has been shifted). The h is around 1200 W/m<sup>2</sup>K on Face 5.

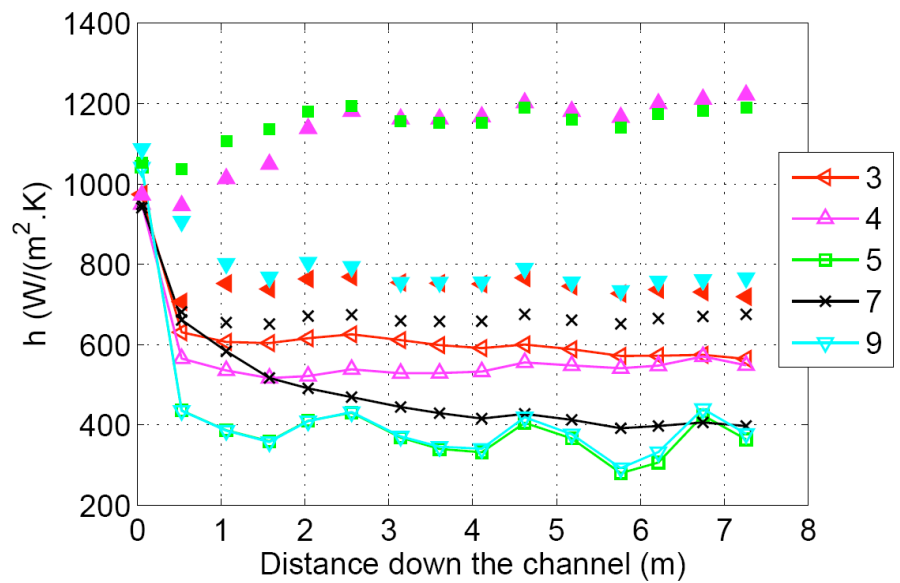


Figure 10: Local heat transfer coefficient (h) of arrowhead passages for NoCF (markers with solid line) and CF (markers only). The results presented for surfaces 3, 4, 5, 7 and 9.

#### 4. Conclusions

CFD analyses have been carried out to investigate the effect of cross flow (or horizontal flow) on the temperature of a moderator brick in an AGR. The study is based on a comparison of two simulations: One is a no cross flow (NoCF) case, which is without explicit consideration of the cross flow. The other is a cross flow (CF) simulation which explicitly simulates the cross flow.

The main conclusions of the present study can be summarized as follows:

- Cross flow (CF) causes significant reduction in brick temperature. The reduction increases as the gas flows down the moderator cooling passages, reaching the maximum around 4m to 6m and reducing afterwards. At any brick cross section, the reduction is strongest facing the incoming CF, and lowest facing the outgoing CF. The reduction is slightly lower on the brick inner surface than on the brick outer surface, being the highest in the key/keyway clearances.
- The reduction of brick temperature in CF is mainly caused by two mechanisms. Firstly, there is a significant cross flow in the key/keyway clearances in the CF case, which results in strong heat transfer from the surfaces forming those clearances. Secondly, the cross flow causes the peak of the axial velocity to shift away from the centre of the arrowhead passage towards the cross-flow downstream side. As a result, the effectiveness of heat transfer on the surfaces of the arrowhead passage next to the upstream of the cross flow is reduced, but it is enhanced on the surfaces close to the outlet of the cross flow. The downstream heat transfer enhancement penetrates into the key/keyway clearances and the heat transfer coefficient may increase by up to 3 times at these locations. The re-distribution of the axial velocity by cross flow contributes to the enhancement of heat transfer.

## 5. References

- [1] J.L. Head and A.N. Kinkead, "Graphite fuel element structures for high temperature gascooled reactors", Nuclear Engineering and Design, Vol. 18, 1972, pp. 115-144.
- [2] S. He and J. Gotts, "A computational study of the effect of distortions of the moderator cooling channel of the Advanced Gas-cooled reactor", Nuclear Engineering and Design, Vol. 235, 2005, pp. 965-982.
- [3] M. Kim, S. Yu, H.J. Kim, "Analyses on fluid flow and heat transfer inside Calandria vessel of CANDU-6 using CFD", Nuclear Engineering and Design, Vol. 236, Issue 11, 2006, pp. 1155-1164.
- [4] E. Studer, A. Beccantini, S. Gounand, et al., "CAST3M/ARCTURUS: A coupled heat transfer CFD code for thermal–hydraulic analyzes of gas cooled reactors", Nuclear Engineering and Design, Vol. 237 (15-17), 2007, pp. 1814-1828.
- [5] P.K. Hutt, N. Gaines, M.J. Halsall, M. McEllin and R.J. White, "The UK core performance code package", Nuclear Energy, British Nuclear Energy Society, Vol. 30, 1991, pp. 291-298.
- [6] M.T. Nicholls, "Brick dimensions for the PANTHER Function GAS REACTOR CORE TEMPERATURE for Heysham2/Torness", BE report EPD/AGR/REP/0506/98, 1998.
- [7] Fluent, 2003. Fluent 6.1.22 user's guide.
- [8] T. Maruyama and M. Harayama, "Neutron irradiation effect on the thermal conductivity and dimensional change of graphite materials Journal of Nuclear Materials", Vol. 195 (1-2), 1992, pp. 44-50.